Reviews

Chemistry of Deltahedral Zintl Ions

Slavi C. Sevov* and Jose M. Goicoechea

Department of Chemistry and Biochemistry, University of Notre Dame, Notre Dame, Indiana 46556

This review focuses on the reactivity of nine-atom deltahedral clusters of group 14, also known as deltahedral Zintl ions, toward various main-group and transition-metal compounds. The redox chemistry of these species and their ability to form oligomers, polymers, and functionalized clusters are discussed, and the cluster geometries, their bonding, and electronic structures are described.

1. Background

Zintl ions were posthumously named after Edward Zintl, who in the early 1930s investigated polyatomic anions of the post-transition metals and semimetals in liquid ammonia.[1] The first known reports of such anions go as far back as 1891, when Joannis observed that liquid ammonia solutions of sodium metal were capable of dissolving elemental lead.[2] It was later found that such solutions could also be obtained by dissolving precursor alloys of the post-transition elements with alkali metals. Diligent work in this area of chemistry by a handful of authors followed;[3] however, it was Zintl who finally determined the composition of many of the anionic species present in such solutions, employing potentiometric titration.[1] Among the anions deduced by these studies were Pb_9^{4-}, Sn_9^{4-}, Sb_7^{3-}, and As_7^{3-}. During the following 55–60 years research on Zintl ions focused primarily on improving their synthesis and on rationalizing subtle differences in their geometries and electronic structures. The most significant breakthrough in the synthesis and crystallization of the aforementioned clusters was the use of macrocyclic polyethers as cation-sequestering agents. Examples are 2,2,2-crypt (4,7,13,16,21,24-hexaoxa-1,10-diazabicyclo[8.8.8]-hexacosane) and 18-crown-6 (1,4,7,10,13,16-hexaoxacyclooctadecane), found to facilitate crystal growth. This resulted in the structural characterization of E_9^{3-}, E_9^{4-}, and E_5^{2-} (E = Ge, Sn, Pb), As_7^{3-}, Sb_7^{3-}, As_{11}^{3-}, Sb_{11}^{3-}, Sb_4^{2-}, and Bi_4^{2-}, as well as several other species (Figure 1).[4] It was realized that bonding in many of these ions cannot be rationalized with simple two-center–two-electron bonds but rather that it is achieved through
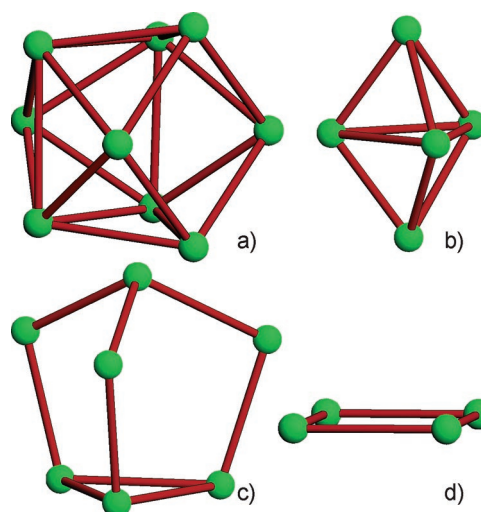

Figure 1. Some of the main-group anionic clusters crystallized from solutions with sequestered alkali-metal cations: (a) E_9^{3-} and E_9^{4-} for E = Ge, Sn, Pb; (b) E_5^{2-} for E = Ge, Sn, Pb; (c) As_7^{3-} and Sb_7^{3-}; (d) Sb_4^{2-} and Bi_4^{2-}. Clusters of silicon with shapes that correspond to those in (a) and (b) were isolated recently.

delocalized electrons. Thus, the ions of group 14 were found to be structurally and electronically analogous to the cagelike boranes:[5] i.e., deltahedral clusters with delocalized bonding that follow Wade's rules for electron counting.[6] For example, E_9^{4-} species are nido clusters with $2n + 4 = 22$ cluster-bonding electrons (each group 14 vertex provides 2 electrons) that can be described either as monocapped square antiprisms or as distorted tricapped trigonal prisms.

Zintl's name is also associated with the so-called Zintl phases, namely saltlike polar intermetallics of a very electropositive s element and a more electronegative p-block metal or semimetal. Until several years ago the two categories of Zintl ions and Zintl phases were thought to be unrelated. However, the discovery of the Zintl phase Cs_4Ge_9 (Figure 2), containing exactly the same Ge_9^{4-} clusters as the Zintl ions characterized

(1) (a) Zintl, E.; Goubeau, J.; Dullenkopf, W. *Z. Phys. Chem., Abt. A* **1931**, *154*, 1. (b) Zintl, E.; Harder, A. Z. *Z. Phys. Chem., Abt. A* **1931**, *154*, 47. (c) Zintl, E.; Dullenkopf, W. *Z. Phys. Chem., Abt. B* **1932**, *16*, 183. (d) Zintl, E.; Kaiser, H. *Z. Anorg. Allg. Chem.* **1933**, *211*, 113. (e) Zintl, E.; Harder, A. Neumayr, S. *Z. Phys. Chem., Abt. A* **1931**, *154*, 92.

(2) (a) Joannis, A. *C. R. Hebd. Seances Acad. Sci.* **1891**, *113*, 795. (b) Joannis, A. *C. R. Hebd. Seances Acad. Sci.* **1892**, *113*, 587. (c) Joannis, A. *Ann. Chim. Phys.* **1906**, *7*, 75.

(3) (a) Kraus, C. A. *J. Am. Chem. Soc.* **1907**, *29*, 1571. (b) Smyth, F. H. *J. Am. Chem. Soc.* **1917**, *39*, 1299. (c) Peck, E. B. *J. Am. Chem. Soc.* **1918**, *40*, 335. (d) Kraus, C. A. *J. Am. Chem. Soc.* **1922**, *44*, 1216. (e) Kraus, C. A. *Trans. Am. Electrochem. Soc.* **1924**, *45*, 175. (f) Kraus, C. A. *J. Am. Chem. Soc.* **1925**, *47*, 43.

(4) For recent reviews see: (a) Corbett, J. D. *Chem. Rev.* **1985**, *85*, 383. (b) Corbett, J. D. *Struct. Bonding* **1997**, *87*, 157. (c) Corbett, J. D. *Angew. Chem., Int. Ed.* **2000**, *39*, 670. (d) Fässler, T. F. *Coord. Chem. Rev.* **2001**, *215*, 377.

(5) Muetterties, E. L. *Boron Hydride Chemistry*; Academic Press: New York, 1975.

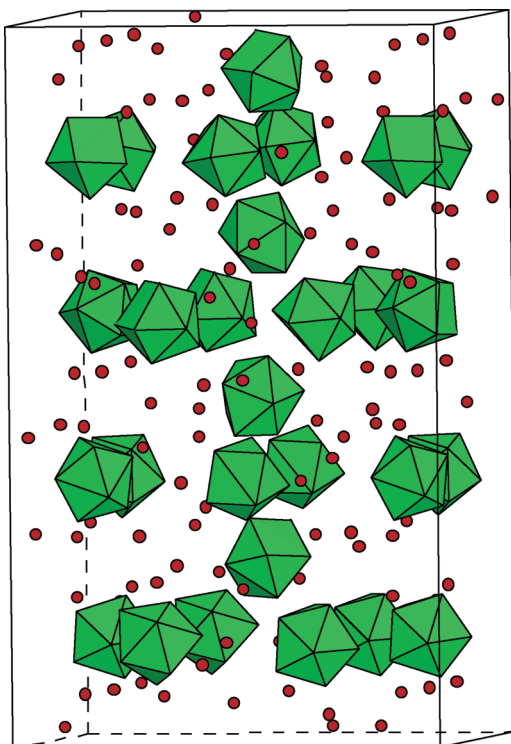(6) Wade, K. *J. Adv. Inorg. Chem. Radiochem.* **1976**, *18*, 1.

Figure 2. Structure of the Zintl phase Cs_4Ge_9 with isolated Ge_9^{4-} deltahedral clusters (green polyhedra) and cesium countercations (red circles). The Ge_9^{4-} clusters have the same overall shape as those crystallized from solutions. Compounds with this stoichiometry are also known for Sn and Pb. All readily dissolve in liquid ammonia and ethylenediamine, yielding the corresponding nine-atom clusters.

from liquid ammonia or ethylenediamine solutions, provided the connection between these two categories.[7] More A_4E_9 and $A_{12}E_{17}$ compounds (where A = alkali metal and E = group 14 element) containing the E_9^{4-} clusters were subsequently characterized ($A_{12}E_{17}$ contains both E_4^{4-} and E_9^{4-}).[8] Understanding this relationship assisted in the recent isolation of the first silicon Zintl ions Si_9^{3-}, Si_9^{2-}, and Si_5^{2-} from liquid ammonia solutions of the Zintl phase $K_{12}Si_{17}$.[9] Even more recently, yet another novel naked Zintl cluster has been isolated in the form of a 10-atom *closo* bicapped square antiprism of lead, Pb_{10}^{2-}.[10]

The first reactions with deltahedral Zintl ions were simple ligand exchange reactions in which a labile ligand of a transition-metal complex was replaced by a Zintl ion. Thus, Sn_9^{4-} and Pb_9^{4-} can readily replace η^6-arene ligands (L) in $LM(CO)_3$ for M = Cr, Mo, W and form the corresponding transition-metal complexes with Zintl ion substituents, $[Sn_9M(CO)_3]^{4-}$ and $[Pb_9M(CO)_3]^{4-}$.[11] A great deal of interesting discoveries involving deltahedral Zintl ions have been made since, and the following pages provide an overview of the current state of their chemistry.

2. Equilibria in Solution

Nine-atom deltahedral Zintl ions with different charges were reported for the heavier elements of this group: Ge, Sn, and Pb. E_9^{4-} and E_9^{3-} were structurally characterized,[4] while E_9^{2-} was crystallized but the structure was never fittingly determined.[12] The latter crystallizes in hexagonal symmetry and exhibits extensive disorder at the cluster site. Nonetheless, it is clear that there are two cations per cluster, and this indirectly proves the existence of E_9^{2-}. The only structurally characterized E_9^{2-} cluster is the recently reported species of the lighter homologue silicon, Si_9^{2-}.[9b]

We have shown that in the case of germanium (and in all likelihood tin and lead) the three differently charged clusters coexist in solution in complex equilibria with solvated electrons.[13] The first indications for this came from early literature reports of the seemingly arbitrary synthesis of E_9^{3-} and E_9^{4-}: i.e., apparently similar reactions would produce E_9^{3-} or E_9^{4-}. However, a closer look at the synthetic conditions showed that the syntheses often differed in the amount of 2,2,2-crypt added to the reaction mixture. It was realized that this seemingly insignificant factor plays an important role in the crystallization of these species, as one of the roles of the sequestering agent is to provide cations of a size comparable to that of the anionic clusters. The effective size of the complex cation of 2,2,2-crypt with a captured alkali-metal cation is nearly 56 times larger than that of a naked alkali-metal cation (effective radii taken as 1.33 and 5.08 Å for K^+ and $[K(2,2,2-crypt)]^+$, respectively). Thus, an excess of sequestering agent will result in only large cations being available for crystallization with cluster anions. Apparently, four such large cations are too many to pack with E_9^{4-} and the crystalline product is usually E_9^{3-} instead, as in $[A(2,2,2-crypt)]_3E_9 \cdot n(en)$ and $[A(2,2,2-crypt)]_6(E_9)_2 \cdot n(en) \cdot m(tol)$ for E = Ge, Sn, Pb.[14] On the other hand, a deficiency of sequestering agent (by approximately 25%) results in the availability of smaller naked alkali-metal cations, and a combination of three large cations and one small cation can pack well with E_9^{4-} in a crystal lattice, as found in $[A(2,2,2-crypt)]_3$-$[A]E_9$.[15] These observations suggest that E_9^{3-} and E_9^{4-} coexist in solution and that the crystalline product depends on the sizes of the available cations.

These ideas were further supported by the subsequent synthesis of a dimer of Ge_9 clusters, $[Ge_9-Ge_9]^{6-}$ (Figure 3).[16] The dimer was synthesized by reducing even further the amount of 2,2,2-crypt to about a third of that needed for complete sequestering of the alkali-metal cations. The larger amount of

(7) Queneau, V.; Sevov, S. C. *Angew. Chem., Int. Ed. Engl.* **1997**, *36*, 1754.

(8) (a) von Schnering, H. G.; Baitinger, M.; Bolle, U.; Carrillo-Cabrera, W.; Curda, J.; Grin, Y.; Heinemann, F.; Llanos, J.; Peters, K.; Schmeding, A.; Somer, M. *Z. Anorg. Allg. Chem.* **1997**, *623*, 1037. (b) Queneau, V.; Sevov, S. C. *Inorg. Chem.* **1998**, *37*, 1358. (c) Todorov, E.; Sevov, S. C. *Inorg. Chem.* **1998**, *37*, 3889. (d) Hoch, C.; Röhr, C.; Wendorff, M. *Acta Crystallogr., Sect. C: Cryst. Struct. Commun.* **2002**, *58*, 45. (e) Queneau, V.; Todorov, E.; Sevov, S. C. *J. Am. Chem. Soc.* **1998**, *120*, 3263. (f) Hoch, C.; Wendorff, M.; Röhr, C. *J. Alloys Compd.* **2003**, *361*, 206.

(9) (a) Goicoechea, J. M.; Sevov, S. C. *J. Am. Chem. Soc.* **2004**, *126*, 6860. (b) Goicoechea, J. M.; Sevov, S. C. *Inorg. Chem.* **2005**, *44*, 2654.

(10) Spiekermann, A.; Hoffmann, S. D.; Fässler, T. F. *Angew. Chem., Int. Ed.* **2006**, *45*, 3459.

(11) (a) Eichhorn, B. W.; Haushalter, R. C.; Pennington, W. T. *J. Am. Chem. Soc.* **1988**, *110*, 8704. (b) Kesanli, B.; Fettinger, J.; Eichhorn, B. *Chem. Eur. J.* **2001**, *7*, 5277. (c) Eichhorn, B. W.; Haushalter, R. C. *Chem. Commun.* **1990**, 937. (d) Campbell, J.; Mercier, H. P. A.; Holger, F.; Santry, D.; Dixon, D. A.; Schrobilgen, G. J. *Inorg. Chem.* **2002**, *41*, 86. (e) Yong, L.; Hoffmann, S. D.; Fässler, T. F. *Eur. J. Inorg. Chem.* **2005**, 3663.

(12) Belin, C.; Mercier, H.; Angilella, V. *New J. Chem.* **1991**, *15*, 931.

(13) Ugrinov, A.; Sevov, S. C. *Chem. Eur. J.* **2004**, *10*, 3727.

(14) (a) Belin, C. H. E.; Corbett, J. D.; Cisar, A. *J. Am. Chem. Soc.* **1977**, *99*, 7163. (b) Corbett, J. D. *J. Am. Chem. Soc.* **1983**, *105*, 5715. (c) Fässler, T. F.; Hunziker, M. *Inorg. Chem.* **1994**, *33*, 5380. (d) Campbell, J.; Dixon, D. A.; Mercier, H. P. A.; Schrobilgen, G. J. *Inorg. Chem.* **1995**, *34*, 5798. (e) Fässler, T. F.; Huntziker, M. *Z. Anorg. Allg. Chem.* **1996**, *622*, 837. (f) Fässler, T. F.; Schütz, U. *Inorg. Chem.* **1999**, *38*, 1866. (g) Critchlow, S. C.; Fässler, T. F.; Hoffmann, R. *Z. Kristallogr.-New Cryst. Struct.* **2000**, *215*, 139.

(15) (a) Burns, R.; Corbett, J. D., *Inorg. Chem.* **1985**, *24*, 1489. (b) Campbell, J.; Dixon, D. A.; Mercier, H. P. A.; Schrobilgen, G. J. *Inorg. Chem.* **1995**, *34*, 5798.

(16) (a) Xu, L.; Sevov, S. C. *J. Am. Chem. Soc.* **1999**, *121*, 9245. (b) Hauptmann, R.; Fässler, T. F., *Z. Anorg. Allg. Chem.* **2003**, *629*, 2266. (c) Suchentrunk, C.; Daniels, J.; Somer, M.; Carrillo-Cabrera, W. Korber, N. *Z. Naturforsch.* **2005**, *60b*, 277.
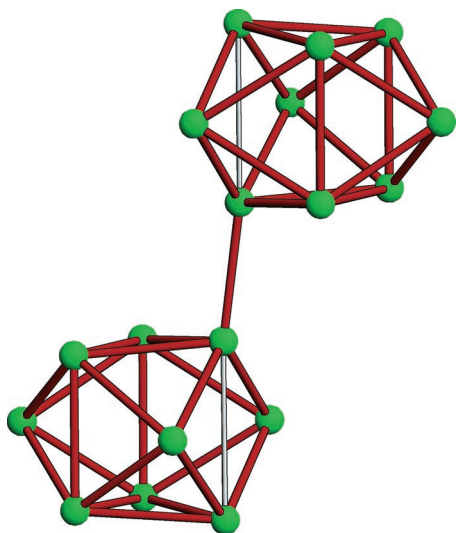
Figure 3. The first example of interconnected deltahedral clusters, the $[Ge_9-Ge_9]^{6-}$ dimer isolated in $[K(2,2,2\text{-crypt})]_2Cs_4[Ge_9-Ge_9]$. The bond between the two clusters is a normal two-center−two-electron Ge−Ge bond of 2.488(2) Å along the elongated edges of each cluster (shown in gray).

available naked cations stabilizes the dimer in the crystalline $[K(2,2,2\text{-crypt})]_2K_4[Ge_9-Ge_9]$.[16b] Use of other sequestering agents in insufficient amounts also yields the dimeric species, as seen in $[Rb(\text{benzo-18-crown-6})]_2Rb_4[Ge_9-Ge_9]$ and $[K(18\text{-crown-6})]_2K_4[Ge_9-Ge_9]$.[16b] A similar effect can be achieved by using large cations that do not fit inside the sequestering agent, such as Cs^+ in the mixed-cation compounds $[K(2,2,2\text{-crypt})]_2Cs_4[Ge_9-Ge_9]$ and $[K(18\text{-crown-6})]_3Cs_3[Ge_9-Ge_9]$.[16a,b] The intercluster bonds in the dimers are normal two-center−two-electron Ge−Ge single bonds.

The discovery of the $[Ge_9-Ge_9]^{6-}$ dimer had two very important consequences. First, it corroborated that differently charged clusters coexist in solutions and their "capture" in crystalline solids depends on the size and shape of the available cations. The second and much more significant consequence was that it contradicted the common belief that such clusters could not add exo-bonded substituents. The deltahedral cluster anions of group 14 were always considered to be so highly reduced that most common laboratory reagents were expected to oxidize them completely to elemental precipitates. In the dimer, however, each cluster plays the role of an exo-bonded substituent to the other cluster, and as such the exo bond is a normal localized bond analogous to the B−H exo bonds in classical cagelike boranes.[5] This new result was quickly reinforced by the discovery of a chain of interconnected Ge_9 clusters $[-(Ge_9^{2-})-]_\infty$ in $[K(18\text{-crown-6})]_2Ge_9\cdot(en)$[17] (Figure 4) and later in $[K(\text{diaza-18-crown-6})]KGe_9\cdot3(en)$,[18] $[Rb_2(2,1,1\text{-crypt})_2]Ge_9\cdot(en)$,[19] and $[-(Hg-Ge_9)-]_\infty$ in $[K(2,2,2\text{-crypt})]_2\text{-}(HgGe_9)\cdot2(en)$.[20] The clusters in these chains have not just one but two exo bonds to neighboring clusters (or to two linear two-coordinate Hg atoms in $[-(Hg-Ge_9)-]_\infty$). Note that the charge per cluster is 2−, which suggests that the dianionic Ge_9^{2-} species are also present in these solutions in addition to Ge_9^{4-} and
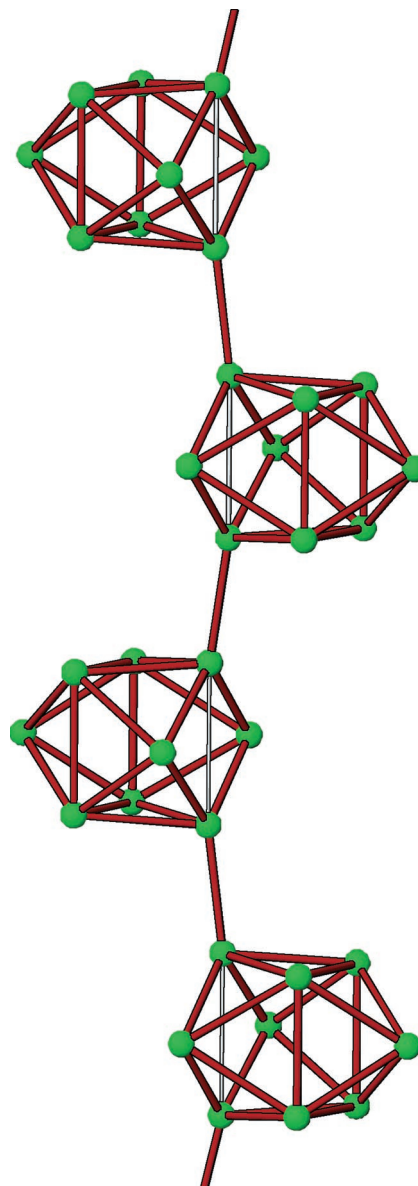

Figure 4. Fragment of the infinite chain of two-bonded Ge_9 clusters with a formal charge of 2− per cluster characterized in $[K(18\text{-crown-6})]_2Ge_9\cdot(en)$. The intercluster bonds are normal two-center−two-electron Ge−Ge single bonds of 2.486(1) Å along the elongated edges of each cluster (shown in gray).

Ge_9^{3-}. It also corroborates the previously mentioned concept that the size and shape of the available cations determine which of these species crystallize from the equilibria present in solution. Further and more detailed studies of solutions of the K_4Ge_9 precursor in ethylenediamine confirmed the coexistence of the three differently charged Ge_9 clusters by a series of cocrystallization experiments.[13] The conclusion is that these species are in equilibria between themselves and solvated electrons: i.e., $Ge_9^{4-} \rightleftarrows Ge_9^{3-} + e^-(\text{solv})$ and $Ge_9^{3-} \rightleftarrows Ge_9^{2-} + 2e^-(\text{solv})$. These equilibria are analogous to the equilibrium between an alkali metal and its cation and solvated electron that occurs in ethylenediamine and liquid ammonia: i.e., $K \rightleftarrows K^+ + e^-(\text{solv})$. It is very likely that the same equilibria or parts of them exist for the nine-atom clusters of the other elements of this group: i.e., Si_9, Sn_9, and Pb_9. We have studied the electrochemistry of Si_9 in pyridine and DMF, and the corresponding CV curves clearly show the Si_9^{2-}/Si_9^{3-} redox pair (Figure 5).[9b]

(17) Downie, C.; Tang, Z.; Guloy, A. M. *Angew. Chem., Int. Ed.* **2000**, *39*, 338.

(18) Downie, C.; Mao, J.-G.; Parmer, H.; Guloy, A. M., *Inorg. Chem.* **2004**, *43*, 1992.

(19) Ugrinov, A.; Sevov, S. C. *C. R. Chim.* **2005**, *8*, 1878.

(20) Nienhaus, A.; Hauptmann, R.; Fässler, T. F. *Angew. Chem., Int. Ed.* **2002**, *41*, 3213.
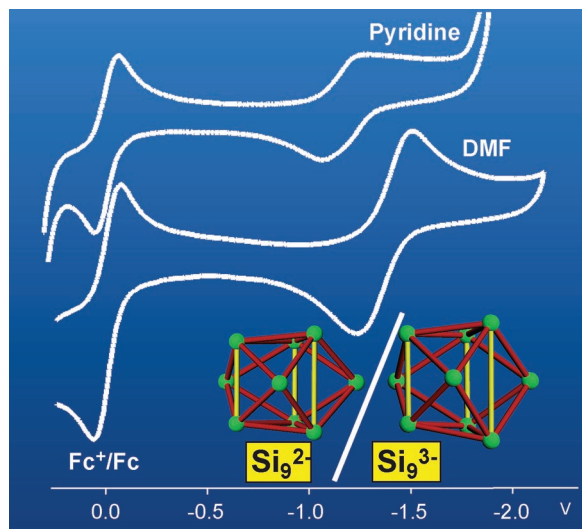
Figure 5. Cyclic voltamograms of the Si_9^{2-}/Si_9^{3-} redox pair in DMF and pyridine with ferrocene as an internal standard, showing a quasi-reversible single-electron process that occurs at -1.37 and -1.17 V, respectively.

3. Geometry and Electronic Structure

The geometry and corresponding electronic structure of the nine-atom clusters are perfectly suited for handling different charges without large structural distortions. In other words, the differently charged species interconvert from one to another without the need for much energy. The overall geometry of the clusters is that of a tricapped trigonal prism (Figure 6). Interestingly enough, most of the distances remain nearly constant for the differently charged clusters E_9^{n-}. These include the 6 distances within the triangular bases of the trigonal prism (top and bottom triangles A$-$A$-$A in Figure 6) and the 12 distances between the three capping atoms and the atoms that form the trigonal prism (distances A$-$B in Figure 6). This means that the triangular bases of the trigonal prism together with the triangular faces attached via common edges to these bases (all shown as filled red triangles in Figure 6) are rigid panels that do not change with the cluster charge. The only significant change is the height of the trigonal prism: i.e., some or all three of the vertical A$-$A distances (dashed vertical lines in Figure 6). These distortions are easy to accomplish without any change to the triangular panels. All that is needed is a little bending around a few "hinges" in the cluster. Such hinges are all of the edges and corners shared between the triangular panels: i.e., the A$-$A edges of the triangular bases of the prisms (shown as ringed binders in Figure 6a) as well as all of the capping atoms B (shown as linked by rings in Figure 6a). Thus, the whole cluster can breathe in and out by bending at those hinges, just like the motion of an accordion, and the only distances that change in this process are the three vertical prismatic edges A$-$A as they elongate and contract correspondingly. Furthermore, this geometry with its three point hinges at the capping atoms allows for independent elongation of the vertical edges: i.e., their variations do not have to be synchronized. This leads to the possibility of having not only clusters with three long or three short edges (Figure 6a,d) but also clusters with one long and two short edges (Figure 6b) as well as clusters with one short and two long edges (Figure 6c). The shape with one long and two short edges (Figure 6b) becomes a special case when the elongated edge (vertical A$-$A in Figure 6b) becomes equal to the distance between the corresponding two adjacent capping atoms (horizontal B$-$B in Figure 6b). The four-corner open face
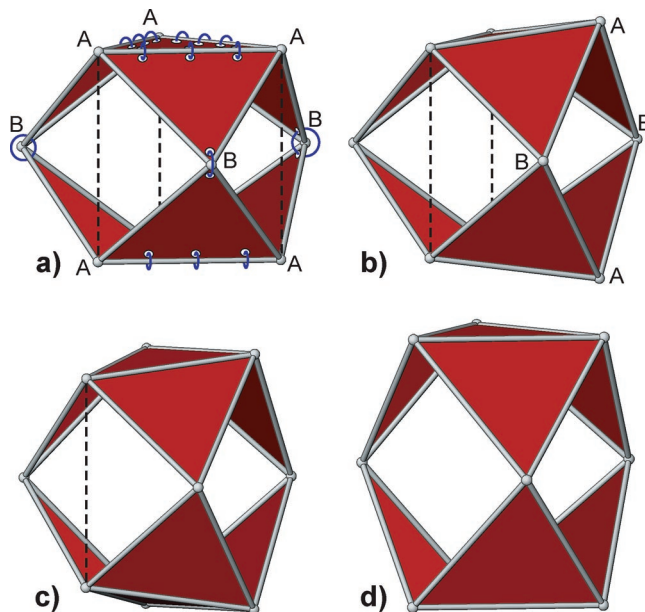

Figure 6. (a) Geometry of the nine-atom clusters, described as derived from an ideal tricapped trigonal prism, where the prism is made of atoms A while atoms B are capping. (b$-$d) The geometries of the observed clusters are derivatives of this shape, where one, two, or three vertical prismatic edges are elongated, as shown in (b)$-$(d), respectively. These distortions are relatively simple. The red triangular panels do not change; they only bend around common edges and corners that act as hinges, as shown in (a).

A$-$B$-$A$-$B in this case becomes a square and the geometry of the cluster approaches that of a monocapped square antiprism with C_{4v} symmetry. Almost all observed geometries, however, deviate from such an ideal symmetry and are better described as tricapped trigonal prisms with one, two, or three elongated prismatic edges. The monocapped square antiprism geometry corresponds to a nido cluster that is derived from a 10-atom closo species with the shape of a bicapped square antiprism where one of the capping atoms is missing (the atom would have capped the A$-$B$-$A$-$B square face in Figure 6b).

The greatest impact of this highly flexible cluster geometry is on its electronic structure. The top three frontier molecular orbitals of the cluster are made predominantly of p_z orbitals (Figures 7 and 8, with z being along the vertical 3-fold axis of the trigonal prism). The orbital with the highest energy (Figures 7a and 8a) is π-bonding within the bases of the trigonal prism but σ-antibonding between them. The other two orbitals (Figures 7b,c and 8b,c) are semidegenerate and opposite in bonding to the first orbital: i.e., they are π-antibonding within the bases of the prism and σ-bonding between them. Evidently, these three orbitals will be most strongly affected by the elongation and contraction of the cluster. Thus, elongation of one or more of the vertical prismatic edges reduces the antibonding character of the highest energy orbital but also reduces the bonding character of one or both of the other two. This phenomenon is directly related to the cluster charges. Clusters with short edges will have a very antibonding first orbital (Figures 7a and 8a) that is high in energy and empty, as is the case for Ge_9^{2-}. The same orbital is lowered in energy when one or more edges are elongated and becomes the HOMO for Ge_9^{3-} and Ge_9^{4-} occupied by one or two electrons, respectively. This geometric plasticity and the resulting electronic flexibility are responsible for the equilibria between the clusters with different charges and solvated electrons that were discussed above.
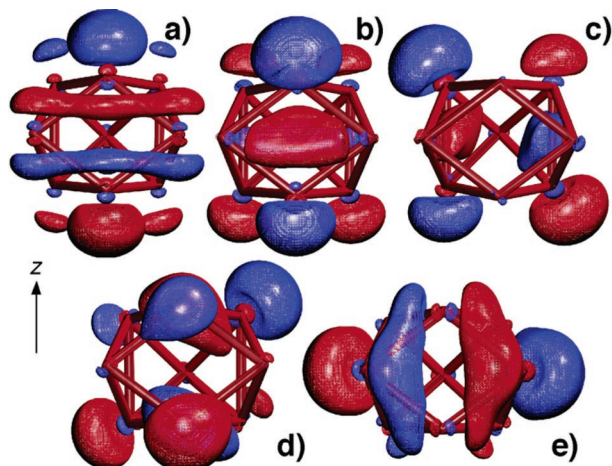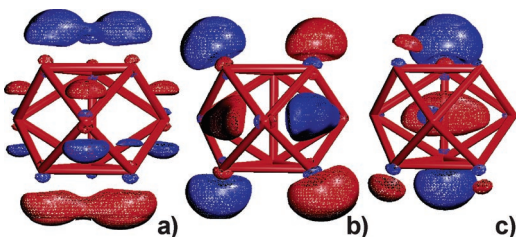
Figure 7. The top five frontier molecular orbitals of a Ge$_9$ cluster with the shape of a tricapped trigonal prism (vertical 3-fold axis) with one elongated edge (the one in front). The top three orbitals (a)−(c) are made up predominantly of p$_z$ atomic orbitals. The orbital shown in (a) is the LUMO for Ge$_9^{2-}$ and HOMO for Ge$_9^{4-}$. It is π-bonding within the triangular bases of the trigonal prism but σ-antibonding between them. The two orbitals in (b) and (c) are semidegenerate. They are π-antibonding within the bases of the prism but σ-bonding between them. The (d) and (e) orbitals have the proper symmetry for π-interactions with an eventual tenth vertex capping the open face in front. Orbital (b) can provide σ-interactions with such a vertex.

Figure 8. The top three frontier molecular orbitals of Ge$_9$ with the shape of a tricapped trigonal prism (vertical 3-fold axis) with two elongated edges: the two in front. Exactly as for the cluster with one elongated edge (Figure 7), they are also made predominantly of p$_z$ atomic orbitals and correspond directly to the orbitals shown in Figure 7a−c. Similarly, the orbital in (a) is π-bonding within the triangular bases of the trigonal prism but σ-antibonding between them. The two orbitals in (b) and (c) are semidegenerate, π-antibonding within the bases of the prism, and σ-bonding between them.

The two orbitals below the orbitals discussed above are shown in Figure 7d,e for the cluster with one elongated edge. These two orbitals are filled and have the appropriate symmetry for π-overlap (vertical and horizontal in Figure 7d,e, respectively) with suitable orbitals from an eventual tenth vertex that would cap the corresponding open face, as in [Sn$_9$M(CO)$_3$]$^{4-}$ and [Pb$_9$M(CO)$_3$]$^{4-}$ for M = Cr, Mo, W (discussed in section 6).[11] The cluster orbital that participates in the corresponding σ-overlap is the one shown in Figure 7b. Thus, these three filled orbitals overlap with three empty frontier orbitals at the transition-metal fragments and provide 6 electrons in order for the latter to satisfy the 18-electron rule.

4. Oligomerization

The existence of the [Ge$_9$−Ge$_9$]$^{6-}$ dimer (Figure 3) and the [−(Ge$_9^{2-}$)−]$_\infty$ chains (Figure 4), as mentioned in section 2,[16−19] proved possible the substitution of a lone pair of electrons at a
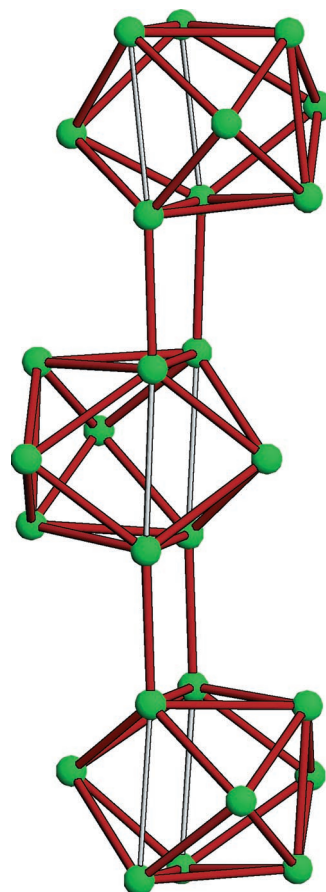

Figure 9. A trimer of Ge$_9$ clusters, [Ge$_9$═Ge$_9$═Ge$_9$]$^{6-}$. Each cluster is a tricapped trigonal prism with two elongated prismatic edges (shown in white). The clusters are bonded along these elongated edges with pairs of parallel intercluster bonds that are longer than normal two-center−two-electron Ge−Ge bonds. Electronically, the bonding in the whole trimer should be viewed as delocalized.

germanium vertex with an exo bond to another cluster. This suggested that exo bonds to other groups might be possible as well. The first exploratory reactions were carried out with triphenylphosphine and triphenylarsine, with the hope of attaching the corresponding groups −PPh$_2$ and −AsPh$_2$ to the germanium clusters. These reactions, however, did not produce functionalized clusters. Instead, they resulted in the synthesis and isolation of the trimer of clusters [Ge$_9$═Ge$_9$═Ge$_9$]$^{6-}$ in [Rb-(2,2,2-crypt)]$_6$[Ge$_9$═Ge$_9$═Ge$_9$]·3(en) (Figure 9).[21] It was determined that PPh$_3$ and AsPh$_3$ acted as mild oxidizing agents in these reactions, oxidizing the clusters exclusively to Ge$_9^{2-}$ while undergoing reduction to PPh$_2^-$ and AsPh$_2^-$, respectively, and Ph$^-$. The phenyl anion is a very strong base and quickly abstracts a proton from the ethylenediamine solvent to form benzene (confirmed by proton NMR) and the corresponding amide. Later studies employing different oxidants also yielded the trimeric oligomers, corroborating our observations.[22]

It appears that the trimers form when the concentration of Ge$_9^{2-}$ is very high. Note that the 6− charge of the trimer suggests that it is made of three Ge$_9^{2-}$ monomers. In the presence of mild oxidizing agents the equilibria between clusters and solvated electrons are shifted completely toward Ge$_9^{2-}$ simply because the solvated electrons are removed from solution. Naturally, when the concentration of a monomer reaches

(21) Ugrinov, A.; Sevov, S. C. *J. Am. Chem. Soc.* **2002**, *124*, 10990.

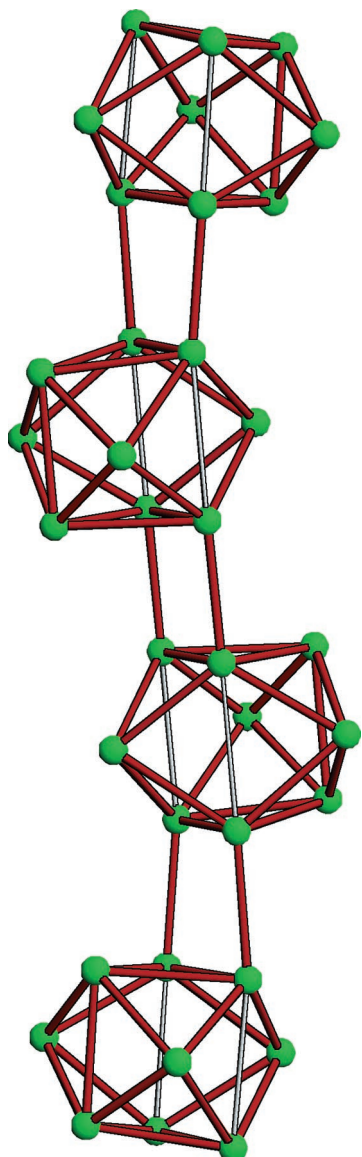(22) Yong, L.; Hoffmann, S. D.; Fässler, T. F. *Z. Anorg. Allg. Chem.* **2005**, *631*, 1149.

Figure 10. A tetramer of Ge_9 clusters, $[Ge_9=Ge_9=Ge_9=Ge_9]^{8-}$. The geometry of the clusters, tricapped trigonal prisms with two elongated edges (shown in gray), and the bonding between them, pairs of parallel bonds as extensions of the elongated prismatic edges, are the same as in the trimer shown in Figure 9.

Figure 11. Two views of the tetramer $[Ge_9=Ge_9=Ge_9=Ge_9]^{8-}$ shown with its environment of "crowned" rubidium cations (purple). The cation−tetramer interactions which stabilize this larger oligomer are shown with dashed lines in (a). It is most likely that this ensemble of a central tetramer surrounded by eight cations and enclosed by the organic crown ether molecules exists intact in solution.

saturation it may form oligomers when it is capable of oligomerization. It seems that when only Ge_9^{2-} clusters are present in solution, the most stable oligomer is the trimer. Of course, the formation of the trimer should involve initial formation of a dimer, but this dimer cannot be the previously discussed single-bonded version $[Ge_9-Ge_9]^{6-}$, as the charge per cluster is 3−. Most likely the clusters in the intermediate dimeric species are bonded by two exo bonds, as in the trimer. Our calculations show that such a dimer will carry an overall charge of 4−, $[Ge_9=Ge_9]^{4-}$, and therefore can be formed by association of two Ge_9^{2-} monomers. This intermediate formation is apparently not very stable and quickly adds another Ge_9^{2-} monomer to form the trimer $[Ge_9=Ge_9=Ge_9]^{6-}$.

It was later discovered that the same trimers could be synthesized by simple oversaturation of the ethylenediamine solution with a precursor: i.e., dissolving as much precursor as possible. Again, this results in a high concentration of Ge_9^{2-} and subsequently in the formation of trimers. Replacing the sequestering agent 2,2,2-crypt with 18-crown-6 in these oxidation and concentration experiments leads to a tetramer of clusters
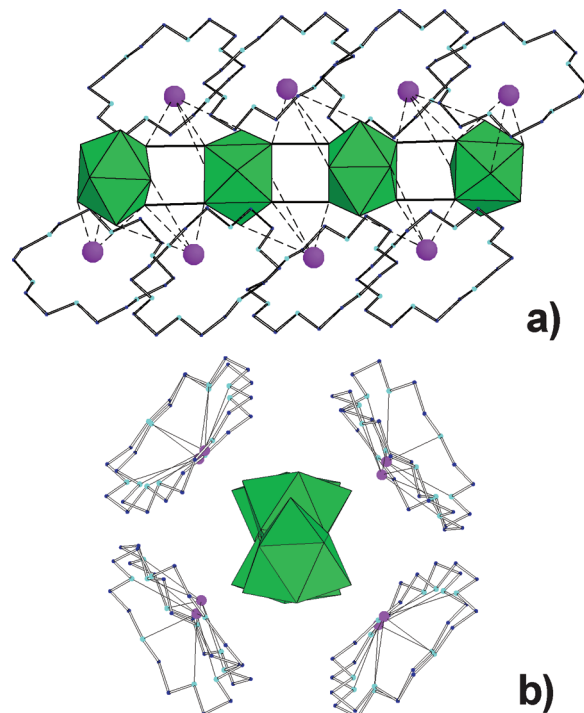
instead.[23] This new oligomer, $[Ge_9=Ge_9=Ge_9=Ge_9]^{8-}$ (Figure 10), initially characterized with $[Rb(18\text{-crown-6})]^+$ countercations,[23] is simply an extension of the trimer by one more cluster that is bonded with the same two-bond mode as the clusters in the trimer. The driving force behind the formation of tetramers instead of trimers is clearly the stabilization effect resulting from the interaction of the oligomer with the exposed alkali-metal cations (Figure 11). Such interactions are not possible with cations captured inside 2,2,2-crypt because they are spherically surrounded by the sequestering agent. Crown ethers, on the other hand, are two-dimensional molecules that leave the cations exposed and available for additional interactions. Note how each cation in Figure 11a interacts with two clusters and assists in their coupling. Furthermore, all eight countercations that balance the 8− charge of the tetramer are involved in such interactions and surround the tetramer. Finally, each countercation is "capped" on the outside with the crown ether, an organic and neutral molecule. Thus, the whole formation is reminiscent of a negatively charged rod, the tetramer, inserted inside a positively charged tube, the eight cations, that are in turn encapsulated inside a neutral organic sheath. It is believed that this "capsule" is the form in which the tetramers exist in solution as well. Following this work, the tetramer was also characterized as a $[K(18\text{-crown-6})]^+$ salt, backing the claim that the interactions between the "exposed" cations and the anionic rod are necessary for the stabilization of such a species.[24]

The two bonds between clusters in the aforementioned trimeric and tetrameric species are clearly not localized two-center−two-electron bonds. They are longer, with distances of

(23) Ugrinov, A.; Sevov, S. C. *Inorg. Chem.* **2003**, *42*, 5789.
(24) Yong, L.; Hoffmann, S. D.; Fässler, T. F. *Z. Anorg. Allg. Chem.* **2004**, *630*, 1977.
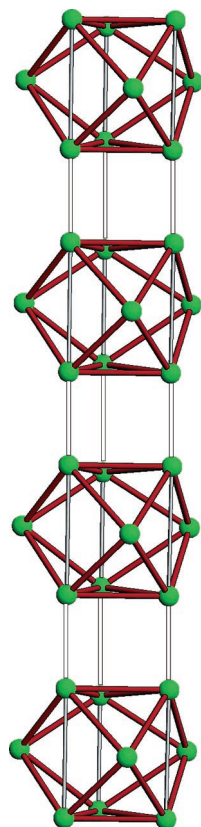
Figure 12. Structure of a proposed tetramer of clusters bonded along all three elongated trigonal-prismatic edges (shown in white). Calculations show that the oligomer is stable with a charge of 6−: i.e., $[Ge_9 \equiv Ge_9 \equiv Ge_9 \equiv Ge_9]^{6-}$.

around 2.65 Å, compared to the single intercluster bonds of about 2.49 Å observed for the dimers. The bonding, using a molecular orbital approach, has been discussed in detail elsewhere.[21,23,25] Suffice to say here that the intercluster bonding is delocalized, similar to the bonding within the clusters. Therefore, the whole oligomer can be viewed as one long cluster made of monomers with delocalized bonding where the delocalization extends to the bonding between them. Note that the intercluster bonds are extensions of two elongated trigonal-prismatic edges in each cluster (shown in gray in Figures 9 and 10). Notice also that the single intercluster bonds in the dimer and the infinite chains are also extensions of such an elongated edge for each cluster (shown in gray in Figures 3 and 4). These observations, in conjunction with the fact that a tricapped trigonal prism has three such edges, naturally leads to the speculation that if clusters can bond along one or two of these edges, they may be able to do so along all three edges. According to calculations, such triply bonded oligomers (Figure 12) carry charges that are lower by 2 than those of the corresponding doubly bonded oligomers. Similarly, these latter species are also lower in charge by 2 than the same-size singly bonded oligomers. For example, tetramers with one, two, and three bonds between the clusters will have charges of 10−, 8−, and 6−, respectively: i.e. $[Ge_9-Ge_9-Ge_9-Ge_9]^{10-}$, the observed $[Ge_9=Ge_9=Ge_9=Ge_9]^{8-}$, and $[Ge_9 \equiv Ge_9 \equiv Ge_9 \equiv Ge_9]^{6-}$. This means that even longer triply bonded oligomers may be possible, because their overall charge would be reasonable. Also, the calculations show that the delocalization is virtually complete in such oligomers with three contacts between the clusters: i.e.,

Figure 13. Structure of $[Ph_2Sb-Ge_9-SbPh_2]^{2-}$ and $[Ph_2Bi-Ge_9-BiPh_2]^{2-}$ (Sb and Bi are shown as yellow spheres). The Ge−Sb and Ge−Bi exo-bond distances correspond to normal single bonds. They are extensions of the elongated trigonal prismatic edge of the cluster (shown in gray).

electronically it is impossible to distinguish the individual clusters from the intercluster regions.

5. Functionalization with Main-Group Fragments

As mentioned above, oxidation of germanium clusters with PPh_3 and $AsPh_3$ exclusively generated the most oxidized clusters Ge_9^{2-} and the corresponding reduced species PPh_2^-, $AsPh_2^-$, and Ph^-. Apparently the two diphenylpnictide anions are inert and do not further attack the clusters. However, this is not the case for the heavier analogues $SbPh_3$ and $BiPh_3$ which, when employed for the oxidation of Ge_9 clusters, lead to clusters with exo-bonded substituents. As a result, the disubstituted clusters $[Ph_2Sb-Ge_9-SbPh_2]^{2-}$ and $[Ph_2Bi-Ge_9-BiPh_2]^{2-}$ (Figure 13) were first isolated.[26] Found later were also the disubstituted dimer $[Ph_2Sb-Ge_9-Ge_9-SbPh_2]^{4-}$ (Figure 14) and small amounts of a cluster functionalized with phenyl and diphenylantimony moieties, $[Ph-Ge_9-SbPh_2]^{2-}$ (Figure 15).[27]

The successful functionalization of the Ge_9 clusters with group 15 substituents hinted at possible similarities in behavior for the corresponding group 14 tetraphenyl reagents EPh_4, where E = Si, Ge, Sn, Pb. Indeed, the reaction with $SnPh_4$ resulted in an analogous disubstituted cluster, $[Ph_3Sn-Ge_9-SnPh_3]^{2-}$, and much smaller amounts of the disubstituted dimer $[Ph_3Sn-Ge_9-Ge_9-SnPh_3]^{4-}$.[13] The same reaction with $GePh_4$ did not produce any product, and this was attributed to the stronger Ge−Ph bond. Instead, a successful reaction was later carried out with the corresponding monohalide, Ph_3GeCl, and led to the analogous germanium-substituted cluster $[Ph_3Ge-Ge_9-GePh_3]^{4-}$.[13]

Generally speaking, the exploration of the redox chemistry of germanium clusters at the time when these reactions were carried out was at a very empirical stage: i.e., there was almost

(25) Pancharatna, P. D.; Hoffmann, R. *Inorg. Chim. Acta* **2006**, *359*, 3776.

(26) Ugrinov, A.; Sevov, S. C. *J. Am. Chem. Soc.* **2002**, *124*, 2442.
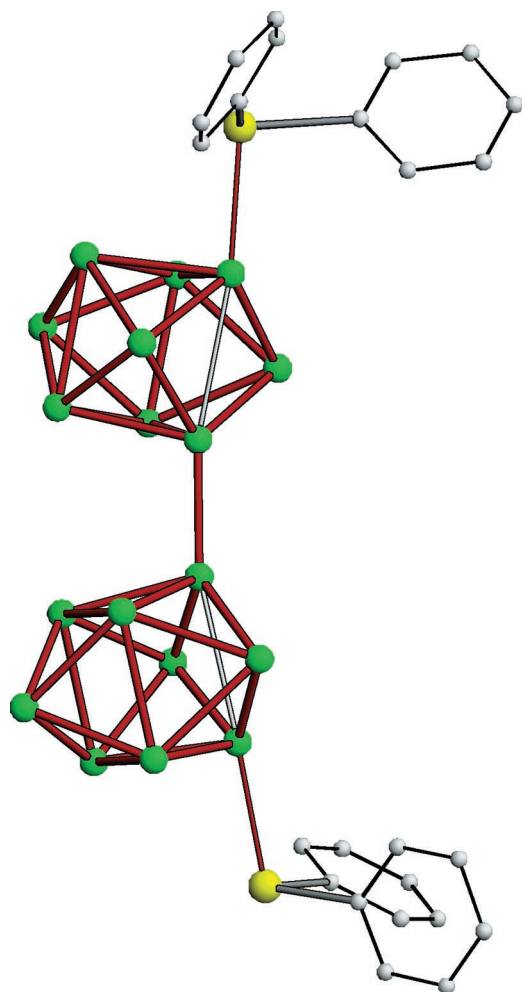(27) Ugrinov, A.; Sevov, S. C. *J. Am. Chem. Soc.* **2003**, *125*, 14059.

Figure 14. Structure of $[Ph_2Sb-Ge_9-Ge_9-SbPh_2]^{4-}$ (Sb is shown as yellow spheres). The intercluster Ge—Ge exo bond and the Ge—Sb cluster exo bonds correspond to single two-center—two-electron bonds. Each cluster has one elongated prismatic edge (shown in gray), and the exo bonds are along that general direction.

no understanding as to why and how the substituents attach to the clusters. Therefore, in order to proceed further, it was necessary to gain some insight into the reaction pathway and, more specifically, into the nature of the species that associate together to form the substituted clusters. The fact that clusters with different charges coexist in equilibria with free and extremely reactive solvated electrons suggests that, in all likelihood, the first step in these reactions involves reduction of the organometallic reagent. Thus, a one-electron reduction of Ph_3GeCl and Ph_4Sn would result in Cl^- and Ph^- anions, respectively. However, it was not clear whether the rest of the molecule would react with the cluster as a radical, i.e., $Ph_3Ge^\bullet$ and $Ph_3Sn^\bullet$, or would undergo additional reduction to form the corresponding anions Ph_3Ge^- and Ph_3Sn^-. In order to resolve this, we dissolved triphenyltin halide in ethylenediamine and reduced it with an excess of elemental potassium in a separate reaction. The resulting Ph_3Sn^- was confirmed by ^{119}Sn NMR.[13] This solution was then added to a solution of germanium clusters. The outcome of this experiment was the same disubstituted cluster $[Ph_3Sn-Ge_9-SnPh_3]^{2-}$ that was previously isolated when Ge_9^{n-} solutions were reacted with Ph_4Sn.[13] The experiment proved, therefore, that the substituents in these cases attach as anionic nucleophiles: i.e., as R_3Sn^-, R_3Ge^-, R_2Sb^-, and R_2Bi^-. All of these species have at least one very nucleophilic lone pair of electrons that can eventually be used
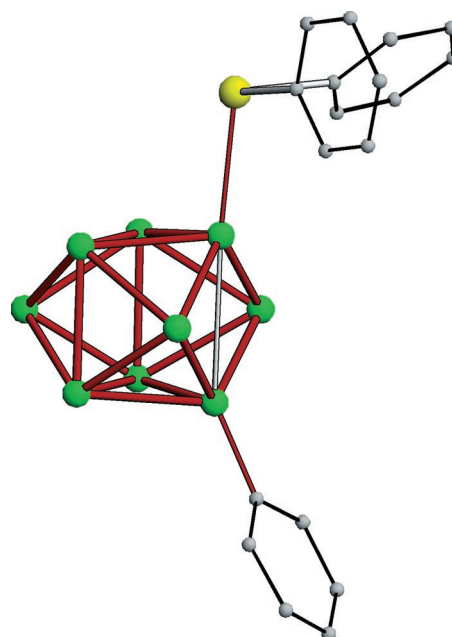

Figure 15. Structure of $[Ph-Ge_9-SbPh_2]^{2-}$ (Sb shown as a yellow sphere). The Ge—Sb and Ge—C exo-bond distances correspond to normal single bonds. While the former is an extension of the elongated trigonal prismatic edge of the cluster (shown in white), the latter is somewhat bent, most likely due to crystal-packing effects.

to form a bond by overlapping with an appropriate empty orbital on the cluster. This, of course, raises the question of whether the clusters can provide such a low-lying, empty, and accessible molecular orbital.

The answer to this question brings us back to the electronic structure of the clusters discussed in section 3 and the orbitals pictured in Figures 7 and 8. Thus, the LUMO of Ge_9^{2-} is such a relatively low-lying, empty, and available molecular orbital. It was already pointed out that this orbital and the two orbitals below it, the HOMO and HOMO-1 for Ge_9^{2-}, are predominantly made up of atomic p_z orbitals. Spatially, the lobes of these orbitals "protrude" outward of the cluster as extensions of the prismatic edges parallel to the 3-fold axis (the z direction). This makes the LUMO conveniently accessible to outside nucleophiles on account of both its relatively low energy as well as its spatial location. Thus, in the first step of the reaction the anionic nucleophiles Nu^- react with Ge_9^{2-} and form $[Nu-Ge_9]^{3-}$. In addition to Ge_9^{2-}, it is possible that Ge_9^{3-} is also involved in similar reactions of addition of a nucleophile. Although the orbital that is empty in Ge_9^{2-} carries one electron in Ge_9^{3-}, its energy is even lower and could eventually accommodate the pair of electrons from the nucleophile by ejecting the extra electron later. The mechanism of addition of the second substituent is not very clear at this stage. It is conceivable that the monosubstituted clusters $[Nu-Ge_9]$ can have different charges, just as the naked Ge_9, and can form similar equilibria with solvated electrons: i.e., $[Nu-Ge_9]^{3-} \rightleftarrows [Nu-Ge_9]^{2-} + e^- \rightleftarrows [Nu-Ge_9]^- + 2e^-$. This will change the occupancy of the frontier orbital and vary its energy. Since this orbital also involves mostly p_z orbitals, its energy position will be again subject to fluctuations of the trigonal-prismatic edges (Figure 16). Thus, the orbital will be empty and low-lying in $[Nu-Ge_9]^-$ (or half-empty in $[Nu-Ge_9]^{2-}$) and will be available to accept an electron pair from one more nucleophile: i.e., $[Nu-Ge_9]^- + Nu^- \rightarrow [Nu-Ge_9-Nu]^{2-}$ (or $[Nu-Ge_9]^{2-} + Nu^- \rightarrow [Nu-Ge_9-Nu]^{2-} + e^-$). An additional strong piece of evidence

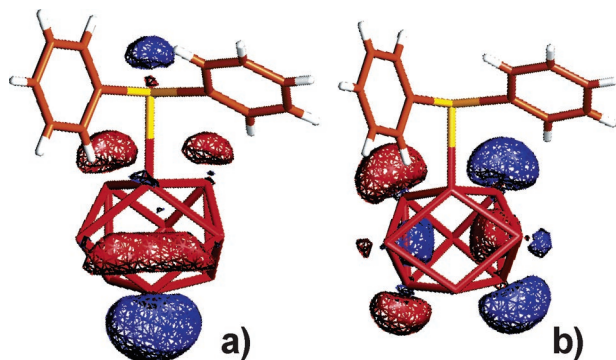**Figure 16.** HOMO (a) and HOMO-1 (b) of [Ph$_2$Sb−Ge$_9$]$^{3-}$. The same two orbitals, made up of mainly atomic p$_z$ orbitals, are the semidegenerate HOMO-1 and HOMO-2 for Ge$_9^{4-}$ (see Figure 7b,c). Note that the HOMO has an external lobe as an extension of the elongated prismatic edge of the cluster, at the other end of which the first substituent is attached. This orbital is empty and is the low-lying LUMO for the proposed [Ph$_2$Sb−Ge$_9$]$^-$ species.
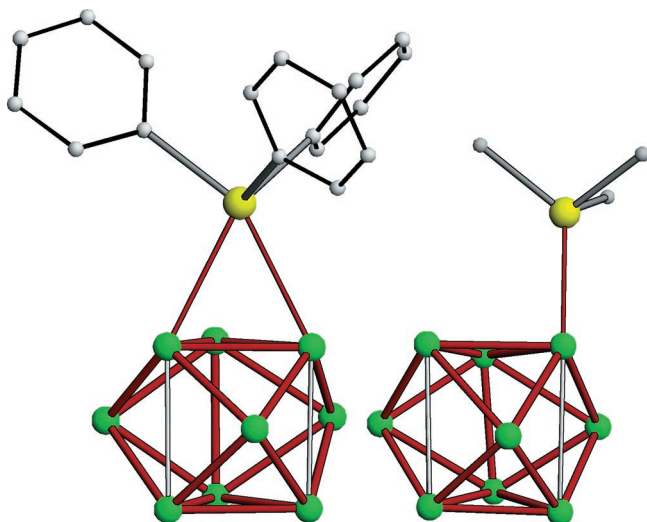

Figure 17. Structures of the monosubstituted species [Ge$_9$−SnPh$_3$]$^{3-}$ (left) and [Ge$_9$−SnMe$_3$]$^{3-}$ (right). Both clusters are tricapped trigonal prisms with two elongated edges (shown in gray). Although the substituent in [Ge$_9$−SnPh$_3$]$^{3-}$ is bridging, the bonding is achieved by a single pair of electrons, just as in the singly bonded SnMe$_3$ in [Ge$_9$−SnMe$_3$]$^{3-}$.

for the involvement of these molecular orbitals is found in the geometry of the resulting substituted clusters, in which the exo bonds are always extensions of the trigonal-prismatic edges: i.e., along the lobes of the cluster orbitals. Without the stereoeffect of these orbitals, one would expect radially pointing exo bonds, as observed in the boranes and carboranes.[5]

This better understanding of the reaction pathway by which these clusters undergo addition of substituents made it possible to rationally design further reactions. Thus, reactions of Ge$_9^{n-}$ clusters with specific amounts of the nucleophiles Me$_3$Sn$^-$ and Ph$_3$Sn$^-$ (prepared by reduction with potassium metal in separate reactions) led to the isolation of the monosubstituted clusters [Ge$_9$−SnMe$_3$]$^{3-}$ and [Ge$_9$−SnPh$_3$]$^{3-}$ (Figure 17),[13] respectively, and the corresponding disubstituted species [Me$_3$Sn−Ge$_9$−SnMe$_3$]$^{2-}$ and [Ph$_3$Sn−Ge$_9$−SnPh$_3$]$^{4-}$, respectively.[13] It should be pointed out that none of the reactions involving preformed anionic nucleophiles of either group 14 or 15 produced the disubstituted dimers (Figure 14) or a phenyl-substituted species (Figure 15). This suggests that their formation might proceed along a different reaction path, perhaps involving radical
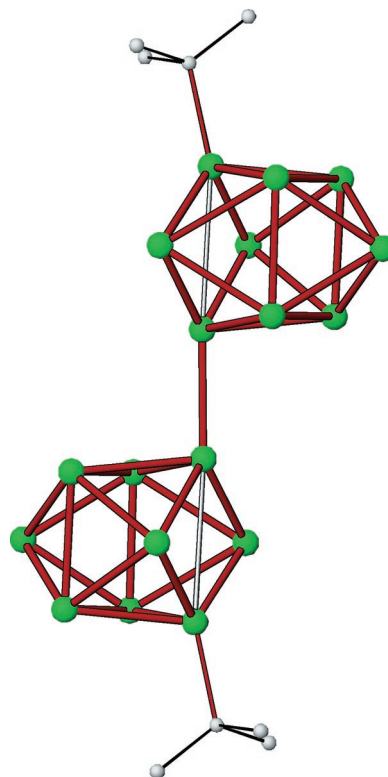

Figure 18. The first alkyl-substituted deltahedral cluster, the *t*Bu-substituted dimer of clusters [(CH$_3$)$_3$C−Ge$_9$−Ge$_9$−C(CH$_3$)$_3$]$^{4-}$.

intermediates. After all, the phenyl substituent in [Ph−Ge$_9$−SbPh$_2$]$^{2-}$ is unlikely to attach as a phenyl anion simply because, as already mentioned, this anion is such a strong base that readily deprotonates the ethylenediamine solvent. On the other hand, the corresponding radical Ph$^\bullet$ may be longer lived and react with the clusters. Such radicals are perhaps generated in a single-electron reduction of a fraction of Ph$_3$Sb that leads to Ph$^\bullet$ + Ph$_2$Sb$^-$ instead of the more likely Ph$^-$ + Ph$_2$Sb$^\bullet$. The reaction of Ph$^\bullet$ with Ge$_9^{2-}$ would result in the radical species [Ph−Ge$_9$]$^{2-}$, which, in turn, might lose an electron to form [Ph−Ge$_9$]$^-$ (same as [Nu−Ge$_9$]$^-$ described above). Both [Ph−Ge$_9$]$^{2-}$ and [Ph−Ge$_9$]$^-$ could react with the available nucleophile Ph$_2$Sb$^-$ and form [Ph−Ge$_9$−SbPh$_2$]$^{2-}$ (Figure 15). The absence of disubstituted dimers [Ph$_2$Sb−Ge$_9$−Ge$_9$−SbPh$_2$]$^{4-}$ in reactions carried out with the anionic nucleophile Ph$_2$Sb$^-$ and their presence in reactions carried out with the neutral starting compound Ph$_3$Sb can be similarly explained. Usage of Ph$_2$Sb$^-$ leads to very low concentrations of [Ph$_2$Sb−Ge$_9$]$^-$ and [Ph$_2$Sb−Ge$_9$]$^{2-}$, as they can be generated only from eventual equilibria with [Ph$_2$Sb−Ge$_9$]$^{3-}$. The presence of Ph$_2$Sb$^\bullet$, on the other hand, leads to high concentration of these low-charged species, which can eventually dimerize, adhering to one or both of the following proposed reaction pathways: [Ph$_2$Sb−Ge$_9$]$^{2-}$ + [Ph$_2$Sb−Ge$_9$]$^{2-}$ → [Ph$_2$Sb−Ge$_9$−Ge$_9$−SbPh$_2$]$^{4-}$ and [Ph$_2$Sb−Ge$_9$]$^-$ + [Ph$_2$Sb−Ge$_9$]$^{3-}$ → [Ph$_2$Sb−Ge$_9$−Ge$_9$−SbPh$_2$]$^{4-}$.

The radical reaction pathway is strongly supported also by some more recent reactions of germanium clusters and alkyl halides. These are perhaps some of the most important substitution reactions, because the clusters are functionalized via direct Ge−C bonds. The product of the reaction with ^{t}BuCl was structurally characterized, while the substituted clusters from reactions with secondary and primary halides have been observed by electrospray mass spectrometry. The product of the reaction with ^{t}BuCl is exclusively the disubstituted dimer [^{t}Bu−Ge$_9$−Ge$_9$−^{t}Bu]$^{4-}$ (Figure 18).[28] Again, the formation of

Figure 19. Overall shape of $[Sn_9M(CO)_3]^{4-}$ and $[Pb_9M(CO)_3]^{4-}$ (M = Cr, Mo, W, shown as a yellow sphere) in which the 9-atom deltahedral clusters act as 6-electron donors and the transition metals satisfy the 18-electron rule.

Figure 20. Structure of $[E_9Zn-Ph]^{3-}$ for E = Si, Ge, Sn, Pb (Zn shown as a yellow sphere).

Figure 21. Frontier orbitals of the ZnPh fragment: (a) an sp hybrid, (b) p_x, and (c) p_y. The sp hybrid σ-overlaps with the cluster orbital shown in Figure 7b, while the p_x and p_y orbitals π-overlap with the cluster orbitals shown in Figure 7d,e.

this specific species strongly supports the radical mechanism for the reaction, i.e., $Ge_9^{2-} + R^\bullet \rightarrow [R-Ge_9]^{2-}$, followed by coupling of these radical monomers. The radical $R^\bullet$ is generated from RX by single-electron reduction to $R^\bullet + X^-$, where the electron is provided by the Ge_9^{n-} equilibria as explained above. Apparently, the bond between the two clusters in these disubstituted dimers is relatively labile under electrospray ionization conditions, and the mass spectra show only the corresponding monosubstituted monomers $[R-Ge_9]$.[28] The organic functionalization of the clusters may provide opportunities toward developing methods for grafting clusters on various halogenated surfaces or incorporating them into halogenated polymers.

6. Functionalization with Transition-Metal Fragments and Insertion of Metal Atoms

As previously mentioned in Section 1, the first functionalization of deltahedral clusters was achieved with the transition-metal fragments $M(CO)_3$, where M = Cr, Mo, W (Figure 19).[11] These reactions are simple ligand-exchange processes where a labile 6-electron ligand L such as mesitylene, cycloheptatriene, or toluene in $LM(CO)_3$ is replaced by Sn_9^{4-} or Pb_9^{4-} clusters, yielding $[E_9M(CO)_3]^{4-}$. Interestingly, there have been no analogous $[Ge_9M(CO)_3]^{4-}$ species characterized to date, an absence which has yet to be accounted for, and presumably arises due to the subtle but important differences in the sizes and electronic properties of the group 14 clusters. The transition-metal atom in $[E_9M(CO)_3]^{4-}$ coordinates to the most open face of the cluster which, in clusters with one elongated prismatic edge, is the squarelike face pictured in Figure 6b and the cluster resembles a monocapped square antiprism. Recent reports suggest that both $[Sn_9M(CO)_3]^{4-}$ and $[Pb_9M(CO)_3]^{4-}$ may be fluxional, with the possibility of the $M(CO)_3$ occupying other positions in the cluster.[11b,e] Independent of the position of the transition-metal fragment, the resulting 10-atom clusters are bicapped square antiprisms (Figure 19) that carry 22 cluster bonding electrons and qualify as closo clusters. The $M(CO)_3$ fragment for M = Cr, Mo, W is isolobal with a $(CH)^{3+}$ group and, therefore, is an electrophile that has three empty orbitals and needs 6 additional electrons.[29] The three empty orbitals have their σ- and two π-matches in the filled cluster orbitals pictured in Figure 7b,d,e, respectively.

We are currently studying the reactivity of deltahedral Zintl ions toward metals at the borderline between transition-metal and main-group elements such as zinc. Reactions of the clusters with diphenylzinc, $ZnPh_2$, result in the loss of one phenyl group
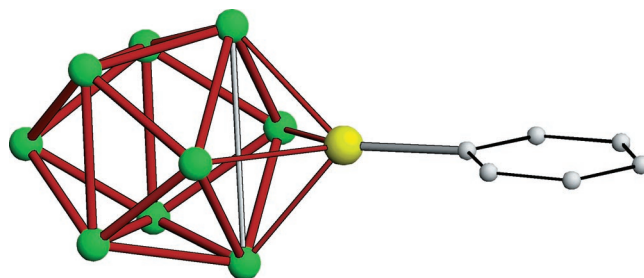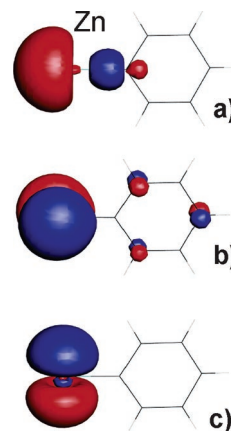
(most likely as a phenyl anion, which subsequently abstracts a proton from the ethylenediamine solvent) and coordination of ZnPh to the open square faces of the clusters (Figure 20).[30] This behavior is analogous to that observed for the transition-metal $M(CO)_3$ fragments, as discussed above. The ZnPh fragment is isolobal with $(CH)^{2+}$ and provides three orbitals and one electron for cluster bonding.[29] The available orbitals at the Zn atom, an sp hybrid and two perpendicular p orbitals (Figure 21), match the available cluster orbitals shown in Figure 7b (σ-overlap) and Figure 7d,e (π-overlap). Thus, the cluster site "attacked" by electrophiles is clearly the open squarelike face formed when one prismatic edge is elongated. It is worth noting the distinction between the site of electrophilic attack observed for species such as ZnPh and $M(CO)_3$ (M = Cr, Mo, W),[11,30] versus the sites of nucleophilic addition of main-group anions (see section 5) along the elongated edges above and below the triangular faces of the trigonal prism (Figure 22).[13,26-28]

Reactions of germanium clusters with nickel complexes showed that not only can the clusters be functionalized with fragments of transition-metal complexes but that they can also be centered with transition-metal atoms. The first such cluster, $[Ni@(Ge_9Ni-PPh_3)]^{2-}$ (Figure 23),[31] was synthesized from a reaction with $Ni(CO)_2(PPh_3)_2$ that was conducted at somewhat elevated temperature. Apparently, the higher temperature strips the nickel atom from its ligands and the carbon monoxide escapes the system. A naked atom then centers the cluster while a second atom caps it. The latter is either already ligated with PPh_3 or acquires the ligand upon cooling. Unlike the previous examples of capped empty clusters where the capping site is

(28) Ugrinov, A.; Petrov, I.; Sevov, S. C. Unpublished results.
(29) (a) Elian, M.; Chen, M. M. L.; Mingos, D. M. P.; Hoffmann, R. *Inorg. Chem.* **1976**, *15*, 1148. (b) Hoffmann, R. *Angew. Chem., Int. Ed. Engl.* **1982**, *21*, 711.

(30) Goicoechea, J. M.; Sevov, S. C. *Organometallics* **2006**, *25*, 4530.
(31) Gardner, D. R.; Fettinger, J. C.; Eichhorn, B. W. *Angew. Chem., Int. Ed. Engl.* **1996**, *35*, 2852. (b) Esenturk, E. N.; Fettinger, J.; Eichhorn, B. *Polyhedron* **2006**, *25*, 521.
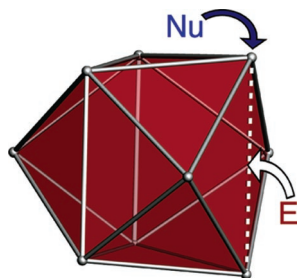
Figure 22. Representation of the sites for nucleophilic (Nu) attack and electrophilic (E) substitution in a Ge_9^{n-} cluster. The dotted line represents an elongated edge of the tricapped trigonal prism (vertical pseudo 3-fold axis). This shape resembles also a mono-capped square antiprism where the open square face is the site for the electrophilic substitution.
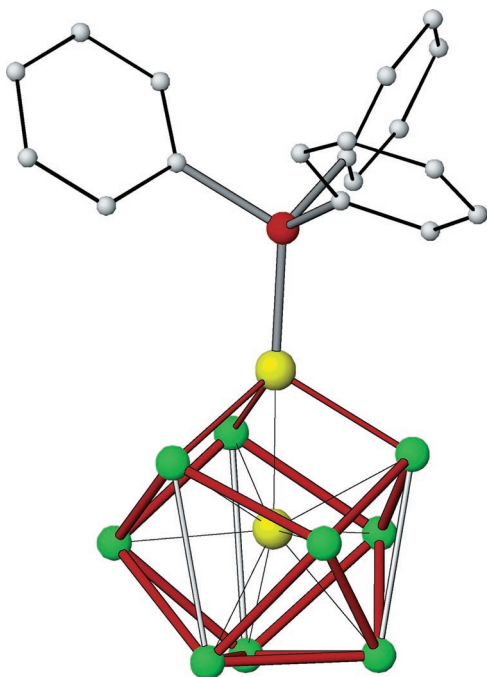

Figure 23. Structure of $[Ni@Ge_9Ni-PPh_3]^{2-}$ (Ni shown in yellow and P in red). The Ni-centered Ge_9 cluster is a tricapped trigonal prism (vertical 3-fold axis) in which the upper triangular base of the prism is capped and forced open by the $Ni(PPh_3)$ fragment.

the open square face (Figures 19, 20, and 22), this centered cluster is capped at one of the two triangular bases of the tricapped trigonal prism. Furthermore, the capped triangular base is forced open, losing its Ge–Ge bonding (Figure 24). Most likely, this distortion occurs in order for the capping nickel atom to become equidistant from the central nickel atom, as are the remaining nine germanium atoms of the cluster. This grants the cluster a spherical shape, and the capping nickel atom participates fully and equally in the delocalized cluster bonding, as do the germanium atoms (Figure 24). The Ni–L fragment is isoelectronic and isolobal with the Cr, Mo, and W tricarbonyl fragments $M(CO)_3$ and, therefore, provides three empty orbitals and no electrons for cluster bonding. The central nickel atom is also a zero-electron donor because of its d^{10} closed-shell configuration. Thus, the cluster $[Ni@(Ge_9Ni-PPh_3)]^{2-}$ has 20 cluster-bonding electrons and qualifies as a capped closo cluster with $2n$ electrons ($n = 10$). A cluster with exactly the same shape and charge, $[Pt@(Sn_9Pt-PPh_3)]^{2-}$, was found for tin when Sn_9 clusters were reacted with $Pt(PPh_3)_4$.[32] The reaction with $Ni(CO)_2(PPh_3)_2$, on the other hand, produced the cluster $[Ni@-$
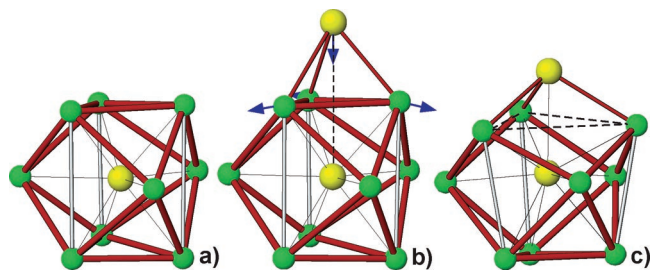

Figure 24. Schematic representation of a centered Ge_9 cluster (a) that is capped at one of the triangular bases of the trigonal prism (b). The distance from the central atom to the capping atom, shown as a dashed line in (b), is significantly longer than the distances to the nine germanium atoms (thin lines). By moving toward the center, the capping atom forces the opening of the triangular base, as shown with blue arrows in (b). This leads to a spherical cluster (c) with all 10 atoms positioned equidistant from the central atom (thin lines). The bonding within the former triangular base of the prism is lost (broken lines in (c)).
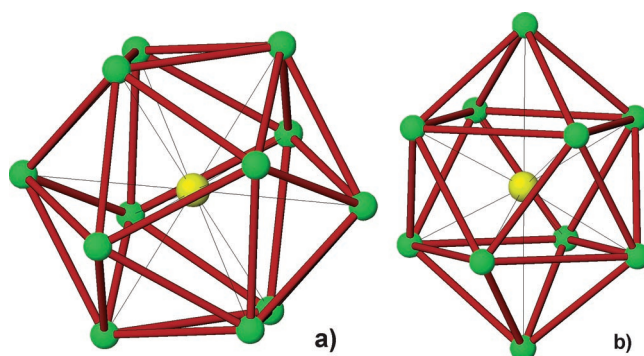

Figure 25. Structures of (a) icosahedral $[Pt@Pb_{12}]^{2-}$ and (b) bicapped-square-pyramidal $[Ni@Pb_{10}]^{2-}$.

$(Sn_9Ni-CO)]^{3-}$, which has a higher charge and the shape of a bicapped square antiprism.[32] This shape suggests a closo species, although the charge corresponds to 21 electrons, which is one electron short of the expected $2n + 2 = 22$. The best way to view this species is as made of Sn_9^{3-}, a known stable empty cluster with 21 cluster bonding electrons, that is centered by a zero-electron-donating Ni atom and capped by another zero-electron donor, a Ni–CO fragment. Capping and/or centering a deltahedral cluster does not change the required number of cluster-bonding electrons, and therefore $[Ni@(Sn_9Ni-CO)]^{3-}$ retains the same number of electrons as the naked empty Sn_9^{3-} cluster.

The nine-atom clusters of lead, on the other hand, behave quite differently in similar reactions capable of generating naked transition-metal atoms. Apparently, they undergo some degree of fragmentation followed by subsequent reassembly around the available naked transition-metal atoms. Thus, reactions of ethylenediamine solutions of K_4Pb_9 with $Pt(PPh_3)_4$ and $Ni-(COD)_2$ (COD = 1,5-cyclooctadiene) produced the Pt-centered icosahedra $[Pt@Pb_{12}]^{2-}$ and Ni-centered bicapped square anti-prisms $[Ni@Pb_{10}]^{2-}$, respectively (Figure 25).[33,34] These clusters are closo deltahedra and carry $2n + 2 = 26$ and 22 cluster-bonding electrons, respectively. As mentioned previously, the interstitial d^{10} atoms do not donate electrons for cluster bonding

(32) Kesanli, B.; Fettinger, J.; Gardner, D. R.; Eichhorn, B. *J. Am. Chem. Soc.* **2002**, *124*, 4779.

(33) Esenturk, E. N.; Fettinger, J.; Lam, Y.-F.; Eichhorn, B. W. *Angew. Chem., Int. Ed.* **2004**, *43*, 2132.

(34) Esenturk, E. N.; Fettinger, J.; Eichhorn, B. W. *Chem. Commun.* **2005**, 247.

and therefore do not alter the cluster electron count. They do, however, play an important role by providing orbitals for overlap with cluster atom orbitals and stabilize further these larger species.

In addition to these species, reaction of lead clusters with $(mes)Mo(CO)_3$ in the presence of a different sequestering agent, diazo-18-crown-6, produces another fractional species, $[Pb_5\{Mo-(CO)_3\}_2]^{4-}$.[35] This is a pentagonal bipyramid with a flat pentagon of Pb_5 and two $Mo(CO)_3$ apices. Its geometry suggests closo species, but the electron count of 14 cluster-bonding electrons is 2 electrons short of the expected 16 electrons for such species. Flat 5-membered rings with greater negative charges such as Si_5^{6-}, Sn_5^{6-}, and Pb_5^{6-} have been characterized in intermetallic phases as well.[36] They are structural and electronic analogues of the cyclopentadienyl anion.

It would be interesting to determine how exactly the new species $[Pt@Pb_{12}]^{2-}$, $[Ni@Pb_{10}]^{2-}$, and $[Pb_5\{Mo(CO)_3\}_2]^{4-}$ assemble from the initial nine-atom clusters: i.e., is it atom by atom or is it via some intermediate fragments. Perhaps, unlike the case for germanium and tin, the lead clusters interact in ethylenediamine solutions by colliding into each other and eventually exchange atoms during such rendezvous. This different behavior is in all likelihood based on the combined properties of the element forming the clusters (electronegativity, size, inert-pair effects, etc.) and the solvent in which the reactions are carried out (dielectric constant, polarity, molecule dimensions, coordinating capability, etc.). Our recent experiments with mixed Ge/Sn clusters indicate that atoms are exchanged between the clusters in solvents such as DMF, DMSO, and acetonitrile, while no exchange occurs in ethylenediamine and pyridine.[37] The major difference between these groups of solvents is in their dielectric constants and, therefore, in their ability to screen charged species such as the anionic clusters. Thus, the solvents with high dielectric constants as DMSO, DMF, and acetonitrile with $\epsilon = 47.24$, 38.25, and 36.64, respectively, provide a medium with lower dielectric permeability that may allow for the ions to collide with each other, while ethylenediamine and pyridine with much lower constants of $\epsilon = 13.82$ and 13.26, respectively, may prevent such interactions between clusters. On the other hand, the difference may be in the coordinating properties of the solvents, with ethylenediamine and pyridine coordinating more strongly to the negative clusters via their more acidic protons at the amine and para position, respectively. The lead clusters are larger, and their negative charge is perhaps more diffuse than in the smaller germanium and tin clusters; thus, the lead clusters may interact with each other even in ethylenediamine, despite the solvent's lower dielectric constant and presumably better coordinating ability.

The research on reactions of germanium clusters with transition-metal complexes was recently renewed by our research group, and many unexpected and exciting new species were discovered. First, the reaction with $Ni(CO)_2(PPh_3)_2$, mentioned above, was carried out again but at room temperature. Under these conditions the result was the empty capped cluster $[Ge_9-Ni-CO]^{3-}$ (Figure 26).[38] Apparently, the carbon monoxide remains in the system at lower temperature and prevents formation of ligand-free nickel atoms that can center the clusters.
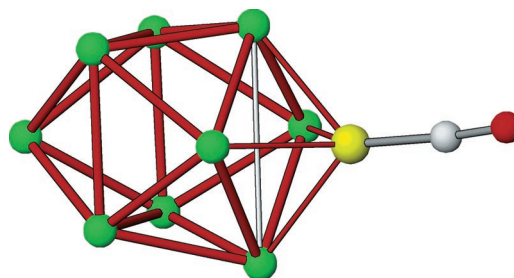

Figure 26. The empty Ni(CO)-capped cluster, $[Ge_9Ni-CO]^{3-}$, synthesized by reacting Ge_9 clusters with $Ni(CO)_2(PPh_3)_2$ at room temperature. The electrophilic Ni(CO) fragment caps the open-square face of the cluster, as observed for $M(CO)_3$ (M = Cr, Mo, W) and ZnPh (Figures 19, 20, and 22). The same reaction when carried out at elevated temperature produces the centered and capped cluster $[Ni@(Ge_9Ni-PPh_3)]^{2-}$, shown in Figure 23. The higher temperature in the latter reaction removes all ligands from some nickel atoms and drives off all carbon monoxide from the system.
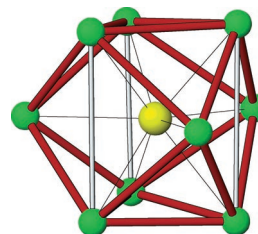

Figure 27. Structure of the centered and uncapped cluster $[Ni@Ge_9]^{3-}$ made by a reaction of Ge_9 clusters with $Ni(COD)_2$. It resembles very closely an empty Ge_9^{3-} cluster with three elongated edges (two of them more so than the third). The central atom causes expansion of the cluster by an average of 0.15 Å per Ge–Ge distance.

This allows for the available Ni–CO electrophile, isoelectronic with $M(CO)_3$ (M = Cr, Mo, W), to interact with the clusters in solution capping the open square face of the cluster, as observed for $M(CO)_3$ and ZnPh. This gives rise to an electron-deficient cluster structurally analogous to the previously described $[E_9M(CO)_3]^{4-}$ and $[E_9ZnPh]^{3-}$ species. After the synthesis of the empty capped cluster $[Ge_9Ni-CO]^{3-}$, the next question was whether the opposite was possible: i.e., the synthesis of a centered cluster without a capping fragment. Needed for such a reaction was a nickel complex in which all ligands were labile, and $Ni(COD)_2$ was chosen. The reaction was successful and produced the centered and uncapped clusters $[Ni@Ge_9]^{3-}$ (Figure 27).[39] The overall shape is the same as that of an empty Ge_9^{3-} (Figure 6), a distorted tricapped trigonal prism, but centered and slightly expanded by about 0.15 Å per Ge–Ge distance. It is likely that the Ni-centered clusters carry different charges, as do the empty Ge_9 clusters, and are in analogous equilibria: i.e., $[Ni@Ge_9]^{4-} \rightleftarrows [Ni@Ge_9]^{3-} + e^-(solv) \rightleftarrows [Ni@Ge_9]^{2-} + 2e^-(solv)$. The centered clusters can also be capped with Ni–CO fragments by reacting them with $Ni(CO)_2$-$(PPh_3)_2$ at room temperature (Figure 28). The new species $[Ni@-(Ge_9Ni-CO)]^{2-}$ (Figure 28c) has the same shape as $[Ni@(Ge_9-Ni-PPh_3)]^{2-}$, a tricapped trigonal prism of germanium that is additionally capped at one of the two triangular bases by the Ni–CO fragment and is compressed along the 3-fold axis so that the capping Ni atom is at the same distance from the central nickel as the germanium atoms.[38] These clusters were, in turn,

(35) Yong, L.; Hoffmann, S. D.; Fässler, T. F.; Riedel, S.; Kaupp, M. *Angew. Chem., Int. Ed.* **2005**, *44*, 2092.

(36) (a) Nesper, R.; Curda, J.; von Schnering, H. G. *J. Solid State Chem.* **1986**, *62*, 199. (b) Todorov, I.; Sevov, S. C. *Inorg. Chem.* **2004**, *43*, 6490. (c) Todorov, I.; Sevov, S. C. *Inorg. Chem.* **2005**, *44*, 5361.

(37) Petrov, I.; Sevov, S. C. Unpublished results.

(38) Goicoechea, J. M.; Sevov, S. C. *J. Am. Chem. Soc.* **2006**, *128*, 4155.

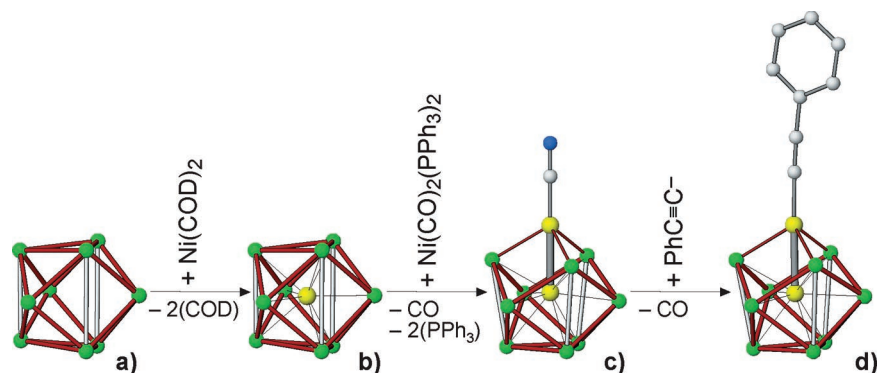(39) Goicoechea, J. M.; Sevov, S. C. *Angew. Chem., Int. Ed.* **2005**, *44*, 2.

Figure 28. Stepwise process of cluster manipulations starting with an empty Ge$_9^{3-}$ cluster (a) and ending with the Ni-centered Ni(C≡CPh)-substituted species [Ni@(Ge$_9$Ni−CCPh)]$^{3-}$ (d). The first step is insertion of a central Ni atom by reaction with Ni(COD)$_2$, which produces [Ni@Ge$_9$]$^{3-}$ (b). Added to this cluster is a capping Ni(CO) fragment by the reaction of [Ni@Ge$_9$]$^{3-}$ with Ni(CO)$_2$(PPh$_3$)$_2$, which results in [Ni@(Ge$_9$Ni−CO)]$^{2-}$ (c). Ligand exchange reaction of the latter with K(C≡CPh) replaces the carbonyl ligand with phenylacetylide in (d).

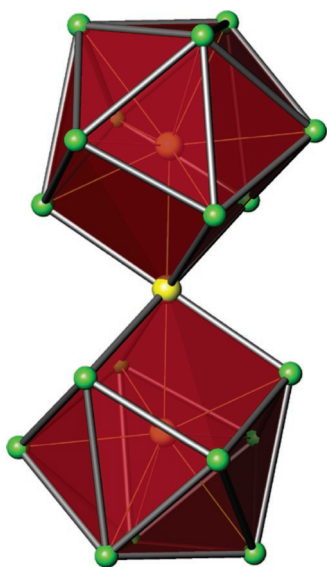**Figure 29.** Structure of [(Ni@Ge$_9$)Ni(Ni@Ge$_9$)]$^{4-}$ (Ni shown as yellow spheres). It can be viewed as made of two Ni-centered Ni-capped clusters that share the capping Ni atom, the central atom in the figure.

used to demonstrate ligand exchange at the capping nickel center. Thus, a subsequent reaction of [Ni@(Ge$_9$Ni−CO)]$^{2-}$ with phenylacetylide anions introduced as K(C≡CPh) exchanged the carbonyl ligand with the phenylacetylide: i.e., [Ni@(Ge$_9$Ni−CO)]$^{2-}$ + (C≡CPh)$^-$ → [Ni@(Ge$_9$Ni−CCPh)]$^{3-}$ + CO (Figure 28).[38] Such an exchange of ligands at one coordination site of a transition metal that is additionally coordinated by a tridentate ligand resembles the well-known chemistry of scorpionate-type metal complexes.[40] In the cluster case, however, the nickel atom is clearly a part of the cluster and participates in the delocalized bonding together with the nine germanium atoms.

The reaction with Ni(COD)$_2$ that resulted in the insertion of nickel atoms in the Ge$_9$ clusters was further studied by exploring different proportions of the reagents. Thus, the reaction with 3 equiv of Ni(COD)$_2$ produced the completely unexpected species of vertex-fused clusters. The new formation, [(Ni@Ge$_9$)Ni(Ni@Ge$_9$)]$^{4-}$ (Figure 29),[39] can be readily rationalized as two Ni-centered and Ni-capped Ge$_9$ clusters that are fused via the capping nickel atom. This arrangement can be viewed also as

a linear trimer of nickel, Ni−Ni−Ni, which is enclosed inside two nine-atom germanium clusters. It was speculated at the time that the process of formation of this species most likely involves one Ni-centered cluster, [Ni@Ge$_9$], and one Ni-centered NiL-capped cluster with a very labile ligand L, [Ni@(Ge$_9$Ni−L)]. The labile ligand is replaced by the Ni-centered cluster in the process. This ligand is most likely a molecule of ethylenediamine from the solvent. This was later supported by the characterization of the species [Ni@(Ge$_9$Ni−en)]$^{3-}$, with the same shape as [Ni@(Ge$_9$Ni−PPh$_3$)]$^{2-}$ and [Ni@(Ge$_9$Ni−CO)]$^{2-}$.[38] Thus, the formation of [(Ni@Ge$_9$)Ni(Ni@Ge$_9$)]$^{4-}$ may be viewed simply as a ligand-exchange reaction in which the ethylenediamine ligand in [Ni@(Ge$_9$Ni−en)]$^{3-}$ is replaced by the Ni-centered cluster [Ni@Ge$_9$]$^{3-}$, as shown in Figure 30. Similar reactions with Sn$_9$ clusters produced the novel species [Ni$_2$Sn$_{17}$]$^{4-}$, in which two Ni-centered clusters are fused by a common Sn vertex.[41]

The reaction of Ge$_9$ clusters with the palladium complex Pd(PPh$_3$)$_4$ produced an even more amazing result, a single-cage deltahedron of 18 germanium atoms with two palladiums encapsulated inside. This species, [Pd$_2$@Ge$_{18}$]$^{4-}$ (Figure 31),[42] represents the largest single-cage deltahedron isolated to date, larger by four vertices than the next largest deltahedron, a 14-atom carborane that was recently reported in the literature.[43] The 2 palladium atoms occupy the foci of a prolate 18-atom germanium cluster with pseudo 3-fold symmetry (vertical in Figure 31). Clearly, these two atoms contribute to the stabilization of such a large cluster. Although they do not provide electrons for cluster bonding, their orbitals overlap with the cluster atom orbitals, especially those radially pointing at the foci, and provide overall stabilization of the cluster molecular orbitals. A spherical cluster with one focus has one radial orbital made of the atomic hybrids pointing in phase at the focus and n tangential cluster-bonding orbitals, therefore requiring $2n + 2$ electrons. The elongated 18-atom cluster, on the other hand, has two radial orbitals due to the two foci and n tangential

(40) Pettinari, C.; Pettinari, R. *Coord. Chem. Rev.* **2005**, *249*, 663.

(41) Esenturk, E. N.; Fettinger, J. C.; Eichhorn, B. W. *J. Am. Chem. Soc.* **2006**, *128*, 12.
(42) Goicoechea, J. M.; Sevov, S. C. *J. Am. Chem. Soc.* **2005**, *127*, 7676.
(43) Deng, L.; Chan, H. S.; Xie, Z. *Angew. Chem., Int. Ed.* **2005**, *44*, 2128.
(44) *Inorganometallic Chemistry*; Fehlner, T., Ed.; Plenum: New York, 1992.
(45) Moses, M. J.; Fettinger, J. C.; Eichhorn, B. W. *Science* **2003**, *300*, 778.
(46) Goicoechea, J. M.; Sevov, S. C. *Angew. Chem., Int. Ed.* **2006**, *45*, 5147.
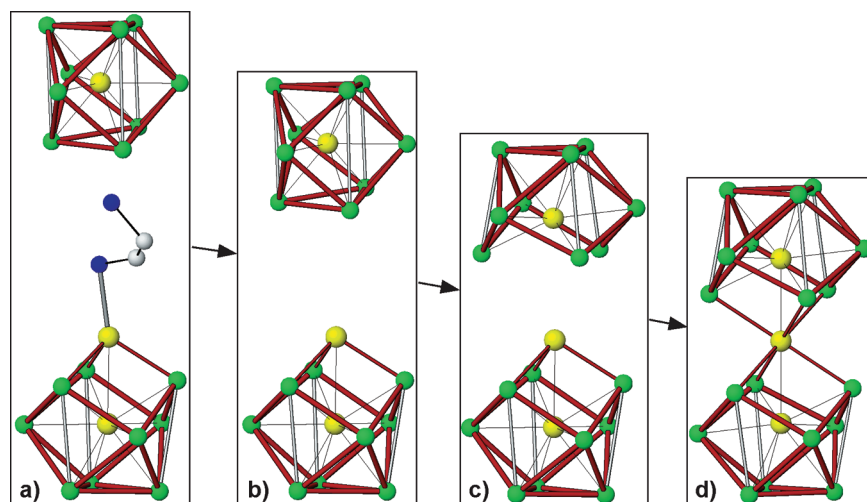(47) Xu, L.; Sevov, S. C. *Inorg. Chem.* **2000**, *39*, 5383.

Figure 30. Schematic representation of the proposed stepwise formation of $[(Ni@Ge_9)Ni(Ni@Ge_9)]^{4-}$ (d) starting from a Ni-centered cluster $[Ni@Ge_9]^{3-}$ and a Ni-centered and Ni(en)-capped cluster $[Ni@(Ge_9Ni-en)]^{3-}$ (a). The labile ethylenediamine ligand of the latter leaves upon approach of the Ni-centered cluster (b). The capping Ni atom interacts with the triangular base of the Ni-centered cluster and the base opens up (c), allowing for Ni−Ge and Ni−Ni interactions (d).
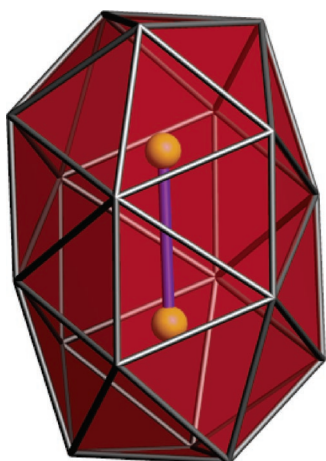

Figure 31. $[Pd_2@Ge_{18}]^{4-}$: the largest single-cage deltahedral cluster. Its elongated shape has two foci occupied by the two Pd atoms. The large deltahedron is stabilized by overlap of the cluster atom orbitals with those of the interstitial transition-metal atoms.

orbitals, thus requiring $2n + 4$ electrons. These $2 \times 18 + 4 = 40$ electrons are provided by the 18 Ge atoms (each a 2-electron donor) and the $4-$ charge of the cluster. Similar to the case for $[(Ni@Ge_9)Ni(Ni@Ge_9)]^{4-}$, this cluster can also be considered as made of two 9-atom clusters, but the clusters are fused to each other without a common transition-metal vertex. They approach each other close enough for direct intercluster Ge−Ge bonds that form the final single-cage deltahedron (Figure 32).

Incorporation of transition metals into deltahedral Zintl clusters has rejuvenated the field in much the same way as their use in borane and carborane chemistry resulted in the birth of inorganometallic chemistry with the discovery of metallaboranes and metallacarboranes.[44] The species discussed above as well as the more complex $[Ni_6Ge_{13}(CO)_5]^{4-}$ can be viewed as nanosize heteroatomic fragments of alloys of the corresponding elements, "molecular alloys".[31b] Such molecular alloys can also be based on group 15 elements, as in $[As@Ni_{12}@As_{20}]^{2-}$,[45] $[Zn@(Zn_8Bi_4)@Bi_7]^{5-}$,[46] $[In_5Bi_4]^{3-}$,[47] and others.

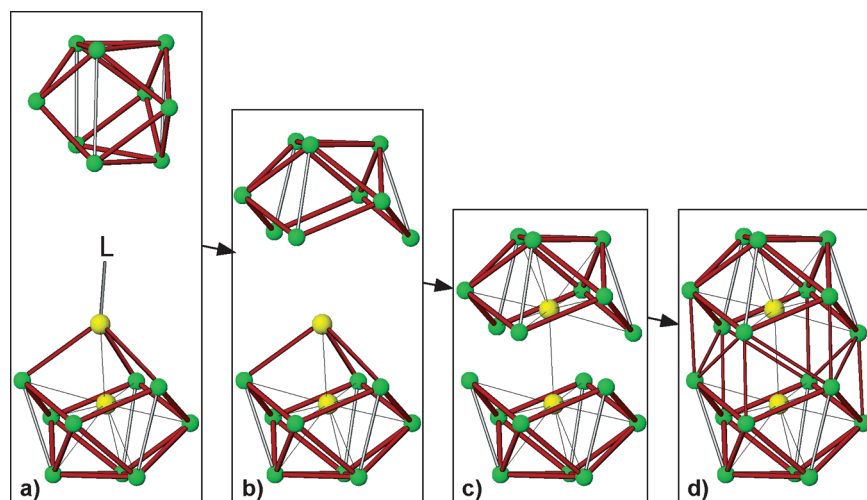**Figure 32.** The single-cage 18-atom germanium cluster in $[Pd_2@Ge_{18}]^{4-}$ (d), viewed as made of two Ge_9 clusters, as shown in this schematic representation. Similar to the case for the $[(Ni@Ge_9)Ni(Ni@Ge_9)]^{4-}$ cluster (Figure 30) this process may involve an unknown Pd-centered, PdL-capped cluster that interacts with an empty Ge_9 cluster (a). The labile ligand L is replaced by the empty Ge_9 cluster, which opens one of its trigonal-prismatic bases upon approaching the capping Pd atom (b). The latter is then inserted in the empty cluster (c). The two Ge_9 clusters get close enough to form bonds between themselves, yielding the final 18-atom single-cage deltahedron (d).

7. Concluding Remarks

The chemical transformations undergone by deltahedral Zintl ions described in this review are based primarily on the controlled oxidation of these highly reduced species, contradicting the long-held belief that such oxidation processes would inevitably lead to cluster decomposition. The wide array of functionalized clusters, oligomers, polymers, and transition-metal and main-group molecular alloys represents intermediate steps on the route to metal and intermetallic precipitates and colloids. Controlled oligomerization and/or interlinking of both empty and centered clusters may provide a convenient approach to a variety of nanoscale species such as spheres, rods, wires, etc. Functionalization with organic moieties via simple reactions with organic halides may be used for incorporating metallic or semiconducting clusters into halogenated polymers and for grafting such species onto various halogenated surfaces. An obvious conclusion is that this field of chemistry is healthy and vigorous, and the fundamental studies of the chemistry of main-group metals and semimetals in negative oxidation states will continue to surprise with many unexpected results.

OM060480O